Supplementary Information

Regioisomerism and π-π interaction Synergistically Enable Mechanical-Ionic Decoupling of Anion Exchange Membranes for Hydrogen Conversion

Pan Li, [a] *Wei Yuan,* [a] *Zhenyi Zhang,* [a] *Lingping Zeng,* [b] *Yuhang Chen,* [a] *Yanting Li,* [a] *Jianchuan Wang,* [*a] *Zidong Wei,* [a]

[a] State Key Laboratory of Advanced Chemical Power Sources, School of Chemistry & Chemical Engineering, Chongqing University, Chongqing 400044, China

[b] Department of Chemical and Biological Engineering, Monash University, Clayton, VIC 3800, Australia.

#These authors contributed to this work equally.

*Corresponding author's E-mail: jxw319@cqu.edu.cn

1. Material and methods

1.1 Materials

5,11-dihydroindolo[3,2-b] carbazole (97%, 5,11-IDCz), 11,12-dihydroindolo[2,3-a] carbazole (97%, 11,12-IDCz), ethyl iodide (97%), p-terphenyl (98%), 1-methyl-4-piperidone (98%), trifluoroacetic acid (TFA, 98 %), trifluoromethanesulfonic acid (TFSA, 98%), iodomethane (CH3I, 98%) were obtained from Adamas. Dichloromethane (CH2Cl2), potassium hydroxide (KOH), tetrahydrofuran (THF), ethyl acetate and methyl sulfoxide (DMSO) were purchased from Chengdu Kelong Reagent. Carbon papers (29 BC, PTFE treated) were purchased from Gore Inc. China. Pt/C (60%) and PtRu/C (75%) were purchased from HESEN Inc. China. IrO2 (85%) was purchased from adamas. All chemicals were used directly without further purification.

1.2 Synthesis of monomer OICZ and PICZ

The synthetic routes to the OICZ are illustrated in Figure S1 (a). 11,12-IDCz (5 g, 19.51 mmol) and KOH (6.57 g, 117.05 mmol) were added to 50 mL THF, stirred at 0 oC for 0.5 h, ethyl iodide (18.26 g, 117.05 mmol) was added dropwise for half an hour. After stirring at room temperature for 10 h, the mixture was poured into ice water to precipitate gray solid. The solid was collected by a suction filtration and washed with distilled water and ethanol. white solid was obtained after drying with a yield of 80%. The same procedure was employed to synthesis of PICZ, with 5,11-IDCz employed as the precursor. as shown in Figure S2 (a).

1.3 Synthesis of QPOTP-15 and QPPTP-15

A typical synthesis procedure of QPOTP-15 is as follows: OICZ (0.46 g, 1.5 mmol), p-terphenyl (1.96 g, 8.5 mmol), 1-methyl-4-piperidone (1.24 g, 11 mmol), and 10 mL of CH2Cl2 were added into a three-necked reactor with mechanical stirring. TFA (1.5 mL) and TFSA (11 mL) were then slowly added at -5 oC. The solution immediately turned dark blue, and was maintained at 0 oC under continuous stirring for 12 h, until the viscosity increased markedly. Subsequently, the polymer solution was precipitated in a 1M KOH solution and was washed several times in DI water until the pH was neutral. Finally, the polymer was dried in a vacuum oven at 80 oC to obtain a white solid POTP-15. Yield: 90%. Then, 1 g of POTP-15 was dispersed in 15 mL of DMSO to form a homogeneous suspension. Next, 1 mL of CH3I was added to the above solution. The quaternization reaction was kept at 30 oC for 24 h in the dark. After the reaction, the polymer solution was precipitated in ethyl acetate and washed thoroughly with deionized water. Finally, the polymer was dried in a vacuum oven at 80 oC for 24 h. Yellow QPOTP-15 solid was obtained with a Yield of 80%. (Scheme 1), The synthesis procedure for QPTP and QPPTP-15 were as the same as that of QPOTP-15.

1.4 Membrane casting and ion exchange

Taking the preparation of QPOTP-15 as an example, QPOTP-15 (0.3 g) was dissolved in DMSO (30 mL) to prepare a homogeneous polymer solution. Subsequently, the polymer solution was collected in a syringe, filtered through a 0.45 um polytetrafluoroethylene (PTFE) filter, and cast onto a clean glass plate. The resulting film was dried in an oven at 80 oC for 24 h to slowly remove the solvent. After drying, the membranes were detached from the glass plate, immersed in 1 M NaOH at 60 oC for 24 h for ion exchange into the OH^- form, and then thoroughly washed with deionized water.

1.5. Characterization

The chemical structures of the monomers and polymers were confirmed by an ^1H NMR (Bruker AVANCE NEO 400 MHz, Switzerland). DMSO-d_6 was used as the solvent with a standard chemical shift of 2.5 ppm. Then, 10% TFA was added to the ^1H NMR samples to eliminate the water peak at 3.3 ppm. The surface morphology and cross-sections of dry AEM samples in I^- form were observed by ESEM (Quattro S, Thermo Fisher Scientific, USA). The samples were fractured in liquid nitrogen and sputtered with gold before analysis. The mechanical properties of dry and wet AEM samples in the OH^- form were measured using a tensile tester (E44.104, MTS, USA) at a tensile rate of 5 mm min^{-1} at room temperature. The free volume in the AEMs was studied by positron annihilation lifetime spectroscopy using a DPLS-4000 Digital Positron Annihilation Lifetime Spectrometer. The gas permeation of dry membranes (in the I^- form) was tested in pure gas systems. Single gas permeation tests for H_2 were carried out at 40 ^oC using the constant-volume/variable-pressure method.

1.5.1. IEC, WU, SR, and ion conductivity (σ)

The experimental IEC values of the AEMs were measured by Mohr titration. The AEMs in the OH^- form were immersed in the HCl solution (30 mL, 0.1 M) for 48 h.

Subsequently, the solution was titrated with a standard NaOH solution (0.1 M) using phenolphthalein as an indicator. The IEC values were calculated using the following equation:

$$IEC = \frac{V_{HCl}C_{HCl} - V_{NaOH}C_{NaOH}}{W_{dry}} \#(1)$$

Where V_{HCl} and V_{NaOH} are the volumes of HCl and NaOH, C_{HCl} and C_{NaOH} are the concentrations of HCl and NaOH, and W_{dry} is the weight of the dry membrane in the OH^- form.

The AEMs in OH^- form was dried in a vacuum oven at 60 °C for 12 h to obtain the dry weight (W_{dry}) and dry length (L_{dry}). The dried samples were then equilibrated in deionized water at different temperatures (25, 40, 60, and 80 °C) for 12 h. After equilibration, the membranes were gently wiped with tissue paper to remove surface water, and immediately weighed and measured to obtain the wet weight (W_{wet}) and wet length (L_{wet}). The water uptake (WU) and swelling ratio (SR) were calculated as follows:

$$WU(\%) = \frac{W_{wet} - W_{dry}}{W_{dry}} \#(2)$$

$$SR(\%) = \frac{L_{wet} - L_{dry}}{L_{dry}} \#(3)$$

The in-plane OH^- conductivity of the AEMs was measured by AC impedance analyzer (Solartron 1287, AMETEK Scientific Instruments, USA) over the frequency range from 0.1 to 100 kHz. Samples in the I^- form were cut into rectangular specimens (1×3 cm) and converted into the OH^- form by soaking in 1 M NaOH at 60 °C for 12 h. The membranes were then thoroughly washed with deionized water to remove residual KOH, fixed in the testing equipment, and immersed in ultrapure water. The distance (L) between the two electrodes was 2 cm. The thickness of the membrane sample was

measured using a Millimar C 1202 profilometer (Mahr GmbH, Göttingen, Germany). In-plane OH^- conductivity (σ) was measured under fully hydrated conditions at elevated temperatures, and the Ohmic resistance (R) of the membrane was recorded. The OH^- conductivity was calculated using the following equation:

$$\sigma = \frac{L}{RA} \#(4)$$

1.5.2. Alkaline stability

The chemical stability of the AEMs was evaluated by immersing the membranes in 1 M NaOH at 80 °C for 1896 h, followed by an accelerated test in 5 M NaOH at 80 °C for an additional 816 h. The OH^- conductivity at 30 °C was recorded at intervals. The chemical structure changes were investigated by ^1H NMR spectra of the membranes before and after the alkaline stability test.

1.5.3. H_2-O_2 single fuel cell

Fuel cell performance of the AEMs was evaluated using a fuel cell test station. Commercial 60 wt% Pt/C (Johnson Matthey) and 70 wt% Pt/Ru/C (Johnson Matthey) were used as the cathode and anode catalysts, respectively. Isopropanol and QPCBP-10% were employed as dispersant and ionomer, with an ionomer-to-catalyst mass ratio of 1:5 (w/w)[1]. The catalyst inks were prepared by sonication for 50 min to obtain homogeneous suspensions. The anode and cathode inks were then sprayed onto opposite sides of the AEM (dry, I^- form) to fabricate catalyst-coated membranes (CCMs). The metal loading was 0.4 mg cm^{-2} for both electrodes, and the effective electrode area was 1 cm^2. Prior to testing, the I^- form membrane was fully converted to the OH^- form by immersion in 1 M NaOH at 60 °C for 12 h. Finally, the CCM was assembled between two carbon paper gas diffusion layers and tested using a fuel cell test system (850e Multi Range, Scribner Associates, USA). Humidified H_2 and O_2 were supplied to the anode and cathode, respectively, at flow rates of 0.5 L min^{-1}.

1.5.4. Anion exchange membrane water electrolysis (AEMWE).

For the AEMWE testing, membrane electrode assemblies (MEAs) based on QPOTP-15, QPPTP-15 and QPTP (30-35 μm, OH^- form) were fabricated. Commercial IrO_2 and Pt/C (60 wt%) were used as the anode and cathode catalysts, respectively. Isopropanol was used as the dispersant, while QPCBP-10 and PAP-BP-80 served as the anode and cathode ionomers, respectively, with an ionomer-to-catalyst mass ratio of 1:4 (w/w)[1]. The catalyst inks were prepared by sonication for 50 min to obtain homogeneous suspensions and then uniformly sprayed onto the membrane surfaces to form CCMs. The CCMs were subsequently immersed in 1 M NaOH at 60 °C for 12 h. The catalyst loadings were 1.5 mg cm^{-2} for the anode and 1.0 mg cm^{-2} for the cathode. Finally, the OH^- form CCM was assembled between two carbon paper gas diffusion layers to form a complete MEA, and 1 M NaOH at 80 °C was used as the feed solution for AEMWE testing.

Theoretical calculations

Gaussian 16 software packages were used to conduct all calculations[2]. All molecular structures were optimized using density functional theory (DFT) M062X with the Def2TZVP basis set[3-5]. There was no virtual frequency in the vibration analysis, which indicated that the corresponding structure was at the minimum position on its potential energy surface, establishing the stability of the optimized compound. The visualization of molecular structures and the extraction of corresponding dihedral angle values from the optimized molecules were performed using the Materials Studio 2023 software.

Table S1. The properties of QPTP, QPOTP-15, and QPPTP-15 membranes.

AEMs	IEC [a] (mmol g^{-1})	WU [b] (%)	SR [c] (%)	σ [d] (mS cm^{-1})	Strength [e] (MPa)	Elongation [f] (%)
QPTP	1.99±0.13	88.7±1.7	18.3±0.3	132.4±3.8	35.0	47.9
QPOTP-15	2.09±0.3	85.4±4.3	12.2±1.9	140.0±11.2	32.8	24.6
QPPTP-15	2.16±0.3	67.8±1.8	6.7±0.2	144.5±8.1	50.0	43.9

[a] Titration ion exchange capacity, [b c] measured at 25 °C, [d] tested at 80 °C, [e f] tested at 25 °C.

Table S2. Performance comparison of this work and reported AEMs.

AEMs	σ (mS cm^{-1})	Strength (MPa)	Ref.
QPPTP-15	144	50	This work
QPTP-TPOTA-6	122.1	16.6	[6]
P(O-$F_{50\%}$-$C_{50\%}$)-GTA	103	12.8	[7]
QP(T-3-Pip)	114.1	20	[8]
PTPQ-Trip	168.8	15.6	[9]
P1-NTP	155	30.6	[10]
QPBF-20	160	50	[11]
b-TPP-30%	259	32.3	[12]

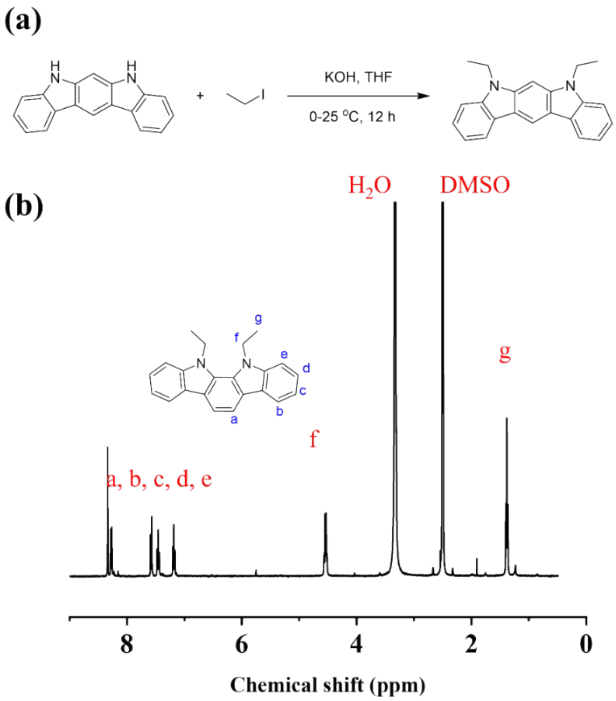

Figure S1. (a) Synthesis route and (b) 1H NMR (400 MHz, DMSO, OICZ) δ 8.34 (s, 2H), 8.28 (d, J = 7.6 Hz, 2H), 7.58 (d, J = 8.1 Hz, 2H), 7.46 (t, J = 7.6 Hz, 2H), 7.19 (t, J = 7.4 Hz, 2H), 4.54 (q, J = 7.0 Hz, 4H), 1.38 (t, J = 7.1 Hz, 6H).

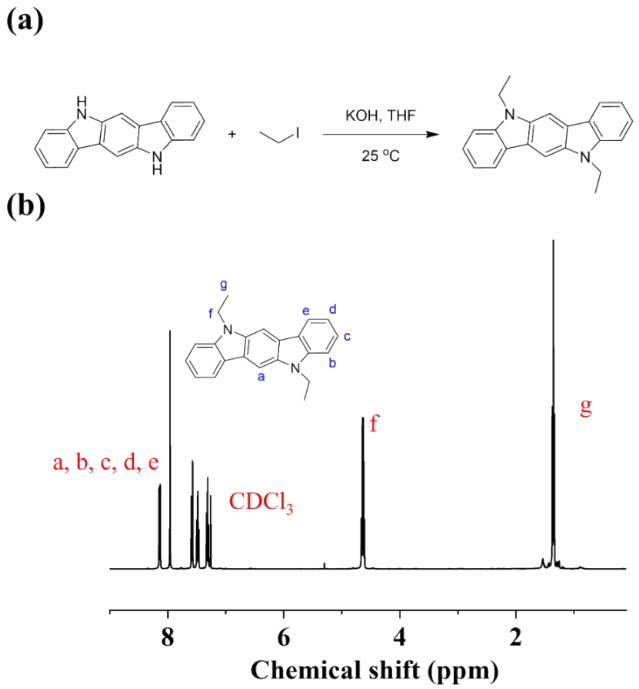

Figure S2. (a) Synthesis route and (b) 1H NMR (400 MHz, $CDCl_3$, PICZ) δ 8.14 (d, J = 7.7 Hz, 2H), 7.96 (s, 2H), 7.63 – 7.43 (m, 4H), 7.31 (t, J = 7.4 Hz, 2H), 4.64 (q, J = 7.1 Hz, 4H), 1.36 (t, J = 7.1 Hz, 6H).

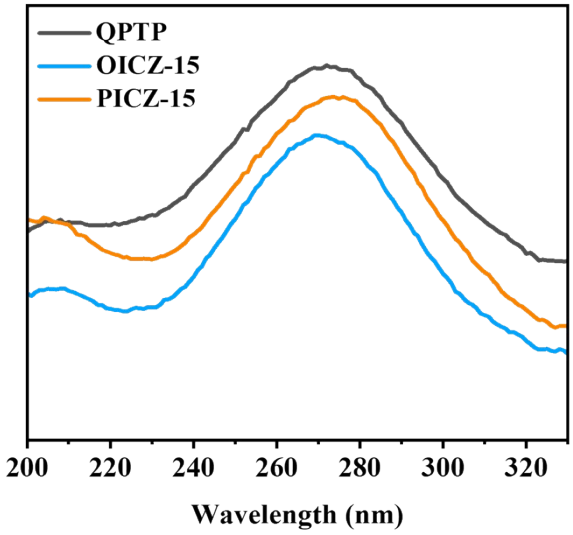

Figure S3. Ultraviolet-visible (UV-vis) absorption spectra of QPTP, QPOTP-15 and QPPTP -15 in thin-film states.

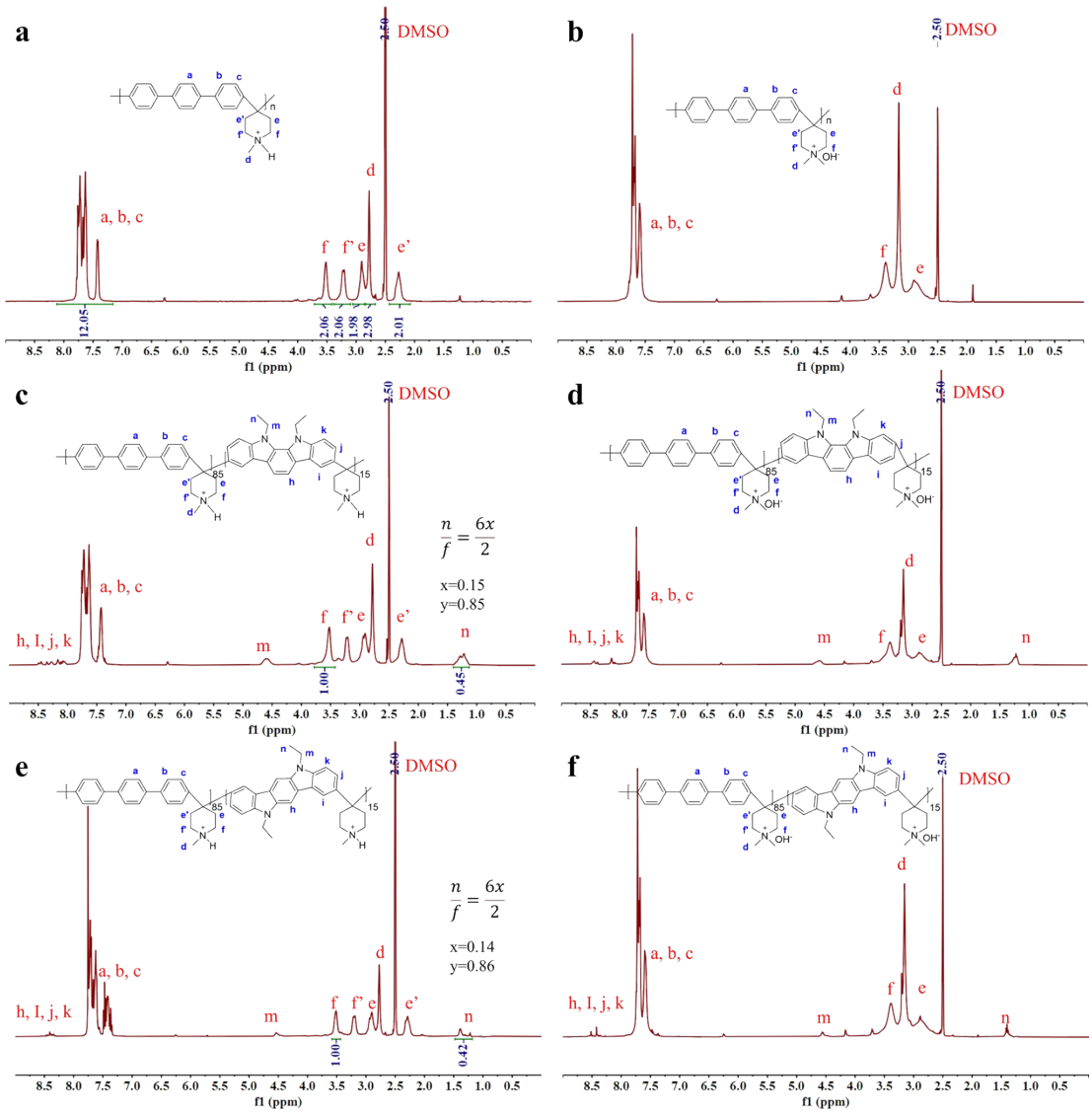

Figure S4. ^{1}H NMR spectrum of (a) PTP, (b) QPTP, (c) POTP-15, (d) QPOTP-15, (e) PPTP-15, (f) QPPTP-15 in DMSO-d6.

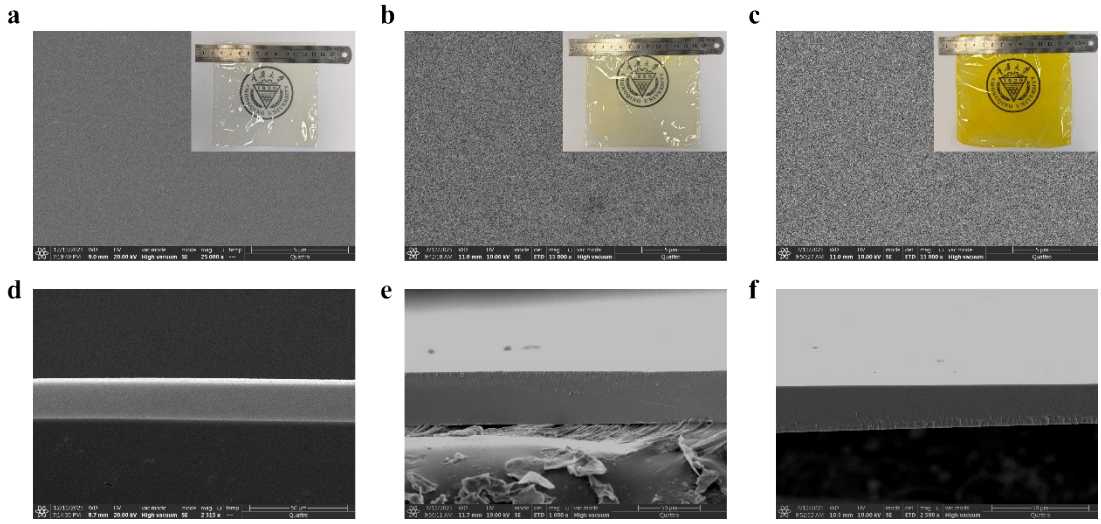

Figure S5. SEM images of the membrane surfaces of (a) QPTP, (b) QPOTP-15, and (c) QPPTP-15, and the corresponding cross-sectional morphologies of (d) QPTP, (e) QPOTP-15, and (f) QPPTP-15.

[1] W. Yuan, L. Zeng, S. Jiang, C. Yuan, Q. He, J. Wang, Q. Liao, Z. Wei, High performance poly (carbazolyl aryl piperidinium) anion exchange membranes for alkaline fuel cells *Journal of Membrane Science* 2022, 657, 120676.

[2] Gaussian 16, Revision A.03, M. J. Frisch, G. W. Trucks, H. B. Schlegel, G. E. Scuseria, M. A. Robb, J. R. Cheeseman, G. Scalmani, V. Barone, G. A. Petersson, H. Nakatsuji, X. Li, M. Caricato, A. V. Marenich, J. Bloino, B. G. Janesko, R. Gomperts, B. Mennucci, H. P. Hratchian, J. V. Ortiz, A. F. Izmaylov, J. L. Sonnenberg, D. Williams-Young, F. Ding, F. Lipparini, F. Egidi, J. Goings, B. Peng, A. Petrone, T. Henderson, D. Ranasinghe, V. G. Zakrzewski, J. Gao, N. Rega, G. Zheng, W. Liang, M. Hada, M. Ehara, K. Toyota, R. Fukuda, J. Hasegawa, M. Ishida, T. Nakajima, Y. Honda, O. Kitao, H. Nakai, T. Vreven, K. Throssell, J. A. Montgomery, Jr., J. E. Peralta, F. Ogliaro, M. J. Bearpark, J. J. Heyd, E. N. Brothers, K. N. Kudin, V. N. Staroverov, T. A. Keith, R. Kobayashi, J. Normand, K. Raghavachari, A. P. Rendell, J. C. Burant, S. S. Iyengar, J. Tomasi, M. Cossi, J. M. Millam, M. Klene, C. Adamo, R. Cammi, J. W. Ochterski, R. L. Martin, K. Morokuma, O. Farkas, J. B. Foresman, and D. J. Fox, Gaussian, Inc., Wallingford CT, 2016.

[3] Y.Zhao and D. G. Truhlar. “The M06 suite of density functionals for main group thermochemistry, thermochemi cal kinetics, noncovalent interactions, excited states, and transition elements: two new functionals and systematic testing of four M06-class functionals and 12 other functionals”. In: *Theor. Chem. Acc.* 2008, 120, 215–41.

[4] F. Weigend and R. Ahlrichs. “Balanced basis sets of split valence, triple zeta valence and quadruple zeta valence quality for H to Rn: Design and assessment of accuracy”. In: *Phys. Chem. Chem. Phys.* 2005, 7, 3297–305.

[5] F.Weigend. “Accurate Coulomb-fitting basis sets for HtoRn”. In: *Phys. Chem. Chem. Phys.* 2006, 8, 1057-65.

[6] Z. Peng,R. Zhang,W. Zhao,Y. Wu,Y. Zhao,J. Yang. Triazine-based multi-heteroatom branching strategy for high-performance anion exchange membranes in water electrolysis. *J. Membr. Sci.* 2026, 738.

[7] Q. Wang,T. Wei,Z. Peng,Y. Zhao,P. Jannasch,J. Yang. High-performance anion exchange membranes based on poly(oxindole benzofuran dibenzo-18-crown-6)s functionalized with hydroxyl and quaternary ammonium groups for alkaline water electrolysis. *J. Colloid Interface Sci.* 2025, 686, 304–317.

[8] Z. Peng,Z. Ren,S. Chen,Y. Zhao,P. Jannasch,J. Yang. Flexibly linked and isomeric piperidinium-based anion exchange membrane with enhanced alkaline stability for durable alkaline water electrolysis. *Int. J. Hydrogen Energy* 2025, 188.

[9] W. Zou,G. Tang,K. Peng,X. Mo,T. Hu,Z. Yang,T. Xu. Quinuclidinium-Based Microporous Anion Exchange Membranes for Water Electrolysis. *Angewandte Chemie-International Edition* 2025, 64 (45), e202514264.

[10] B. Xue,R.-B. Zang,J.-R. Wu,Z. Zheng,J. Yao,Q. He,Z. Wang,P.-N. Liu,J. Yan. Positional Engineering of Ionic Side Chains Enhances π-π Stacking in Poly(m-Terphenylene Alkylene) Anion Exchange Membranes to Address the Conductivity-Stability Tradeoff. *Macromolecules* 2025, 58 (20), 11302–11314.

[11] C. Yang,Y. Huang,W. Song,M. Wu,J. Nie,Y. Wang,L. Wu,X. Ge,T. Xu. Enhanced OH- conductivity and alkaline stability of AEM by pyrene stacking backbone for water electrolysis. *Science China-Materials* 2025, 68 (10), 3657–3666.

[12] C. Yuan,Y. Chen,X. Lu,X. Ma,W. Yuan,X. Zhu,B. Chen,J. Wang,Z. Wei. Reducing hydroxide transport resistance by introducing high fractional free volume into

anion exchange membranes. *J. Membr. Sci.* 2024, 701, 122769.